

Fingerprint Center Point Location Using Directional Field

Y.H. Chan and S.A.R. Abu-Bakar

Universiti Teknologi Malaysia, 81310 Skudai, Johor, Malaysia.

{yhuichan@yahoo.com and syed@fke.utm.my}

Abstract

This paper presents a reliable fingerprint center point (CP) location algorithm for the alignment of fingerprints to construct a shift invariant fingerprint recognition system. The proposed algorithm is based on Alteration Tracking (AT) and CP estimation (CPE). AT is proposed to extract a track that records the transition from one quantized direction to another. CPE is aimed to find the bending point with highest transition of direction from the transition track. This algorithm is tested against fingerprints captured from SAGEM MSO100 optical scanner and the second database from University of Bologna. Experimental result shows that the proposed algorithm is capable of reliably locating fingerprint CP.

1. Introduction

Automatic fingerprint recognition system often faces the problem of fingerprint translation, rotation and distortion during fingerprint acquisition. Two fingerprints from the same individual may suffer from these undesired situations. Hence, CP is used as a pre-processing stage for fingerprints alignment to construct a shift invariant system. Most of the available algorithm for locating a CP is by finding a core point from the directional field based on Poincaré index, such as [1] and [2]. It is due to the fact that Poincaré index is able to locate singular points, thus problem arises for arch fingerprints.

Reference point location algorithm presented in [3] calculates the difference of sine component for orientation field between adjacent regions. [4] presents a simplified method for calculating fingerprint orientation by finding approximate gradients of the image, an intersection of a near zero transition for both approximate gradients in x- and y-axis is obtained from its neighbourhood and its singularity type is determined using derivatives from the two gradient vectors to calculate the angle between them.

In this work, we define CP by using the definition of reference point proposed in [3]. The CP is the point of

maximum curvature of the concave ridges in a fingerprint image [3]. The proposed algorithm in this work is to have a quick access to locate CPs for fingerprints of all classes, i.e. whorl, right, left loop and arch from fingerprint directional field. One CP is estimated for one fingerprint. This paper is organized as follows: Section 2 presents the directional image construction algorithm and grayscale opening operation. Section 3 illustrates AT algorithm. The CPE is explained in Section 4. Section 5 shows the performance of the proposed algorithm and finally conclusions are drawn in Section 6.

2. Fingerprint Directional Field

Based on the work by [5], an input fingerprint image undergoes wavelet transform (WT) using Haar wavelet coefficients $[\frac{1}{2} \ -\frac{1}{2}]$ for high pass filter and $[\frac{1}{2} \ \frac{1}{2}]$ for low pass filter. The second stage WT is done by using expanded coefficients for edge detection similar to Prewitt gradient filter. The expanded coefficients for high pass filter and low pass filter are respectively $[\frac{1}{2} \ 0 \ -\frac{1}{2}]$ and $[\frac{1}{3} \ \frac{1}{3} \ \frac{1}{3}]$. Ridge orientation estimation is

$$\theta_{(r,c)} = \tan^{-1} \left[\frac{W_{vert}^2(r,c)}{W_{hori}^2(r,c)} \right]$$

where $W_{vert}^2(r,c)$ is vertical detail of 2nd stage WT

$W_{hori}^2(r,c)$ is horizontal detail of 2nd stage WT

The directional image is quantized into 8 directions, smoothed using smoothing filter of size 7×7 and then down sampled with a factor of 2. The input fingerprint is $N \times N$ and the obtained directional image is $\frac{N}{8} \times \frac{N}{8}$.

Grayscale opening operation is performed over the directional field to smooth the transition edge between grayscale value 144 representing $+11.25^\circ$ and grayscale value 108 representing -11.25° , and eliminating grayscale values which represent higher value of degree within region of lower value of degree.

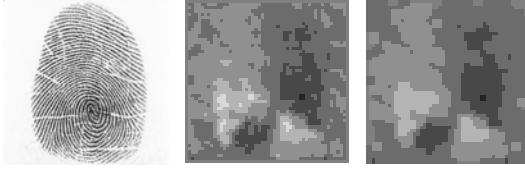


Figure 1. Original fingerprint, directional field and opened directional field (from left to right)

3. Alteration Tracking

A middle alteration track records the transition from $+11.25^\circ$ (grayscale value 144) to -11.25° (grayscale value 108). The middle alteration track is set to -11.25° due to the fact that there is no grayscale value representing 0° . AT is performed within region $M \times M$ at the center of $\frac{N}{8} \times \frac{N}{8}$ opened directional image to ensure that there are enough alteration. Middle alteration track region is valid within region $P \times P$ centered at the opened directional field to ensure that the informative region centered at an estimated CP is of largest possible size $\frac{N}{16} \times \frac{N}{16}$. AT is formed by performing Left Chain Code (LCC). To obtain a starting point of LCC, there is an empirically determined initial condition that needs to be fulfilled. If the track is broken when none of the LCC with alteration track pixel model is able to acquire a track pixel, a continuous initial condition is determined empirically to obtain another starting point of LCC.

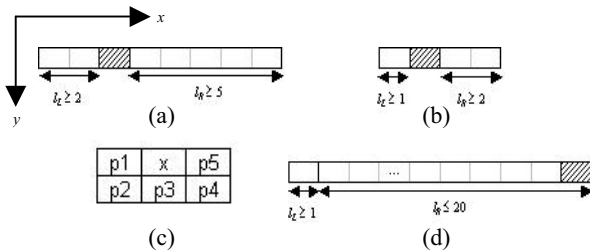


Figure 2. LCC Initial condition, LCC continuous initial condition, LCC and middle alteration track pixel model (from left to right and top to bottom)

The highlighted pixels in Figure 2 are the locations of destination pixels which are of pixel value 108. The initial condition in Figure 2(a) shows that if there are at least 2 pixels ($l_L \geq 2$) to the left of the destination pixel having grayscale value 144 and at least 5 pixels ($l_R \geq 5$) to the right of the destination pixel having grayscale value ≤ 108 , then the destination pixel is the starting pixel for the alteration track. The same applies to the continuous initial condition in Figure 2(b) with $l_L \geq 1$ and $l_R \geq 2$. The continuous starting point is valid only if the x-coordinate absolute difference between the latest alteration track

pixel and the continuous starting point is less than $\frac{M}{2}$ pixels, which is determined empirically. From Figure 2(c), 'x' is the origin of LCC representing (x, y) , and p1 has the highest priority, followed by p2, p3, p4 and p5 in an anticlockwise manner. By placing p1, p2, p3, p4 or p5 according to their priorities to the highlighted destination pixel in Figure 2(d), the selected pixel is a valid alteration track pixel if $l_L \geq 1$ having grayscale value 144, and $l_R \leq 20$ having grayscale value 108. There are additional conditions need to be obeyed by p1 and p5, i.e. p1 is allowed for separating region with grayscale value ≥ 144 at location $(x-l, y-l)$ and region with grayscale value ≤ 108 at location $(x-l, y+l)$; p5 is allowed for separating region with grayscale value ≤ 108 at location $(x+l, y-l)$ and region with grayscale value ≥ 144 at location $(x+l, y+l)$. The separated line segments are linked to form a continuous line. 3 types of middle alteration track are: (a) whorl fingerprints fall into either one of type 1 or 2, (b) right loop has type 1 alteration track, (c) left loop has type 2 alteration track, (d) type 3 represents a nearly straight line that applies to arch and tented arch fingerprints.



Figure 3. Type 1, 2 and 3 middle alteration track (from left to right)

4. Center Point Estimation

CPE is aimed to find the bending point with highest transition of direction for type 1 and 2. CP for type 3 will be discussed towards the end of this section. It is imperative to note that CPs for type 1 and 2 can be detected only if they are within $P \times P$ region of interest (ROI). If there is no CP detected within this region, it is assumed that the particular image is arch or tented arch.

CP locating is done along the middle alteration track. A precise track is the key to successfully estimate a CP. The first step to find a CP candidate is to do scanning from bottom to top and right to left (BTRL) as shown in Figure 4(a) over the middle alteration track. Type 1 CP model as illustrated in Figure 4(b) is sliding in such a way that the highlighted pixel is a pixel on the middle alteration track, pixels at direction northwest (Nw) is at the left side of the track, and pixels at northeast (Ne) and southwest (Sw) are at the right side of the track. The dominant grayscale value for Nw is grayscale value ≥ 144 , whereas the dominant grayscale value for Ne and Sw is grayscale value ≤ 108 . For pixels within the dotted bounding box, i.e. Nwa, Nwb, Nea, Neb, Swa and Swb, must obey the dominant grayscale value. No noise can be

If there is no CP found from the above algorithm, it is possible that the track is not a typical type 1 or 2, but is a variant of them. An example of a variant for type 1 is given for clearance in Figure 5. The last segment of the

Figure 1 consists of four sub-figures labeled (a) through (d).
 (a) A diagram showing a 2D coordinate system with a horizontal x-axis and a vertical y-axis. Two blocks labeled 'BTRL' are shown, each containing three vertical arrows pointing upwards. A curved arrow indicates a path from the top of the first BTRL block to the top of the second BTRL block.
 (b) A diagram showing a sequence of nodes labeled N00 through N36. The nodes are arranged in a grid-like structure. A shaded square node is located at the intersection of the third row and the fourth column. The nodes are arranged in a sequence that follows a path from N00 to N36.
 (c) A diagram showing a sequence of nodes labeled N01 through N28. The nodes are arranged in a grid-like structure. A shaded square node is located at the intersection of the third row and the fourth column. The nodes are arranged in a sequence that follows a path from N01 to N28.
 (d) A diagram showing a sequence of nodes labeled N10 through N38. The nodes are arranged in a grid-like structure. A shaded square node is located at the intersection of the third row and the fourth column. The nodes are arranged in a sequence that follows a path from N10 to N38.



If no CP can be obtained from both type 1 and 2 CP searching, then it can be concluded that the particular directional image is either an arch or a tented arch (type 3). For left and right alteration track tracking, the highlighted pixels in Figure 6 are destination pixels with grayscale value $valuenR$. A left alteration track records the transition from $+33.75^\circ$ ($valuenL=180$) to $+11.25^\circ$ ($valuenR=144$), whereas a right alteration track records the transition from -11.25° ($valuenL=108$) to -33.75° ($valuenR=72$). The left alteration track is set to $+11.25^\circ$ and the right alteration track is set to -33.75° . l_L and l_R obey $valuenL$ and $valuenR$ respectively. The continuous starting point is valid if the x-coordinate absolute difference between the latest alteration track pixel and the continuous starting point is less than $\frac{M}{3} - 1$ pixels, which

is determined empirically. LCC is the same as in Figure 2. By placing p1, p2, p3, p4 or p5 according to their priorities to the highlighted destination pixel in Figure 6, the selected pixel is a valid alteration track pixel if $l_L \geq 1$, and $l_R \leq 9$. There are additional conditions need to be obeyed by p1 and p5, i.e. p1 is allowed for separating region with grayscale value $\geq \text{valuenL}$ at location $(x-1, y-1)$ and region with grayscale value $\leq \text{valuenR}$ at location $(x-1, y+1)$; p5 is allowed for separating region with grayscale value $\leq \text{valuenR}$ at location $(x+1, y-1)$ and region with grayscale value $\geq \text{valuenL}$ at location $(x+1, y+1)$. The distance between left track and right track are examined along the middle track. A point on middle alteration track with smallest distance between left track and right track is decided as the true CP.

5. Experimental Results

An experiment has been carried out using 386 images that obey the assumption that CPs are laid in region $P \times P$ at the center of opened directional images. Figure 7 gives the frequency or number of occurrences of particular Euclidean distance (ED) in pixels between the manually assigned CP and the CP located by the proposed algorithm. From Figure 7, if tolerance is set to a value of 6 pixels, CPs for a total of 374 images from 386 test images are correctly detected, resulting in 96.89% CP detection rate. Due to the fact of lacking arch fingerprint samples, only 2 out of 5 tests have been successful in extracting CP. Although 6 pixels tolerance seems to be significant, from manual observation the difference of ED among fingerprints of the same individual is not distinct, i.e. less than 4 pixels and images for the particular individual are well aligned. We present some results of the proposed CP location in Figure 8 (their corresponding middle alteration tracks are given in Figure 3).

CP detection experiments have been carried out on second database obtained from University of Bologna [6]. The database contains 168 images from 21 fingers (8 items per finger). From 168 images, 8 images are ignored due to poor quality, 3 images are exempted because their CPs are out of ROI, arch fingerprints and 5 fail detections are excluded. Statistical analysis of previous works is obtained from [2], which is given with respect to the original image size. The CP detection algorithm proposed in this work is with respect to 1/8 of original image size. Theoretically speaking, to compare the proposed algorithm with previous works, the distances given in [2] are divided by 8. The image size is 416×416 captured by SAGEM MSO100 optical scanner and 256×256 from second database obtained from University of Bologna. The empirically determined constant values used for testing of both databases are: $M=30$, $P=22$.

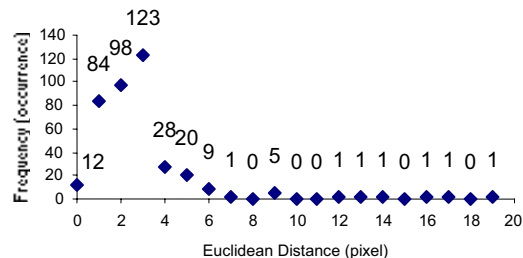


Figure 7. Graph Frequency versus ED

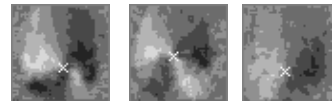


Figure 8. True center points on directional fields

Table 1. Comparison for center point detection algorithm

Test	Average distance from manually detected center point (pixel)
Proposed algorithm	3.89
Algorithm from [2]	1.61
Algorithm from [3]	5.63

6. Conclusions

This paper has presented a fingerprint CP location algorithm based on AT. CP locating is done along the middle alteration track, thus having a quick access to locate fingerprint CPs. Experimental results show that the proposed algorithm is capable of locating fingerprint CP with high accuracy, thus serves as a pre-processing module for fingerprint recognition.

7. References

- [1] A. K. Jain, S. Prabhakar and H. Lin, "A Multichannel Approach to Fingerprint Classification," *IEEE Transactions on Pattern Analysis and Machine Intelligence*, vol. 21, pp. 348-359, 1999.
- [2] N. Kitiyanan and J. P. Havlicek, "Modulation Domain Reference Point Detection For Fingerprint Recognition," *6th IEEE Southwest Symposium on Image Analysis and Interpretation*, March 28-30, 2004, pp. 147-151.
- [3] A. K. Jain, S. Prabhakar, H. Lin and S. Pankanti, "Filterbank-Based Fingerprint Matching," *IEEE Transactions on Image Processing*, vol. 9, pp. 846-859, 2000.
- [4] P. Rämö, M. Tico, V. Onnia and J. Saarinen, "Optimized Singular Point Detection Algorithm For Fingerprint Images," *Proceedings International Conference on Image Processing*, Oct 7-11, 2001, vol. 3, pp. 242-245.
- [5] M. Mohd-Mokji, "Fingerprint Classification And Matching Using Signatures Obtained From Second Stage Wavelet Transform," MEng Thesis. Univ. Teknologi Malaysia, 2002.
- [6] Biometric System Lab (University of Bologna - ITALY), <http://www.csr.unibo.it/research/biolab/>